Permeation of chemisorbed hydrogen through graphene: a flipping mechanism elucidated

Massimiliano Bartolomei [a], Marta I. Hernández, and José Campos-Martínez

Instituto de Física Fundamental, Consejo Superior de Investigaciones

Científicas (IFF-CSIC), Serrano 123, 28006 Madrid, Spain[†]

Ramón Hernández Lamoneda

Centro de Investigaciones Químicas, Universidad Autónoma

del Estado de Morelos, 62210 Cuernavaca, Mor. México

Giacomo Giorgi

Dipartimento di Ingegneria Civile ed Ambientale (DICA),

The University of Perugia, Via G. Duranti 93,

I-06125 Perugia, Italy, CNR-SCITEC, I-06123, Perugia, Italy

(Dated: March 22, 2021)

The impermeability of defect-free graphene to all gases has been recently contested since experimental evidence (see Nature **579**, 229-232 (2020)) of hydrogen transmission through a two-dimensional carbon layer has been obtained. By means of density functional theory computations here we elucidate a flipping mechanism which involves the insertion of a chemisorbed hydrogen atom in the middle of a C-C bond via a transition state that is relatively stable due to a sp^2 rehybridization of the implicated carbon atoms. Present results suggest that transmission for hydrogenated graphene at low local coverage is highly unlikely since other outcomes such as hydrogen diffusion and desorption exhibit quite lower activation enthalpies. However, at high local coverage, with a given graphenic ring tending to saturation, the proposed flipping mechanism becomes competitive leading to a significantly exothermic process. Moreover, for a specific arrangement of four neighboring chemisorbed hydrogen atoms the flipping of one of them becomes the most likely outcome with a low activation enthalpy (about 0.8 eV), which is in the range of the experimental estimation. The effect of charge doping is investigated and it is found that electron

---

[a] Corresponding author, e-mail:maxbart@iff.csic.es

doping can help to reduce the related activation enthalpy and to slightly enhance its exothermicity. Finally, an analysis of corresponding results for deuterium substitution is also presented.

† maxbart@iff.csic.es

1. INTRODUCTION

Two-dimensional materials are being used for developing a new class of membranes for the transport of atoms and molecules at the nanoscale[1]. As these membranes are atomically thin, permeances are expected to become much larger than for thicker materials, and nanopores can be tailored for allowing a large selectivity of the desired species with respect to other molecules in a gas or liquid mixture. Until recently, it has been believed that at ambient conditions, perfect graphene is completely impermeable to even the smallest atoms[2, 3]. For example, by means of Density Functional Theory (DFT) calculations, Miao *et al*[4] found that protons (H^+) and atomic hydrogen (H) need to surmount rather large energy barriers (~ 2.2 and 2.9 eV, respectively) to pass through the middle of the graphenic carbon ring. If it is assumed that these species are initially chemisorbed to graphene, even larger energy barriers were obtained for the flipping of the atoms from one side to the other of the graphene sheet (~ 3.4 and 4.5 eV for H^+ and H, respectively).

Contrarily to previous predictions, in 2014 Hu *et al*[5] reported transport and mass spectroscopy measurements of protons permeating graphene with a much lower activation energy (~ 0.8 eV). These findings inspired numerous studies with the aim to uncover the microscopic mechanisms underlying these observations[6–14], including the possible role of small defects in enhancing the proton conductivity[15–17]. It must be noted that, in those experiments, the graphene membrane is in contact with an aqueous medium (hydrated Nafion of HCl solution) where protons are mainly attached to water as hydronium (H_3O^+)[8]. Removal of a proton from hydronium and a subsequent penetration of the former through graphene as a free particle seems unfeasible due to the large proton affinity to water[8, 9]. However, transferring a proton from hydronium to the graphene carbon atoms leading to its chemisorption is a more likely process[10]. Recently, some of us have studied[18] a possible mechanism responsible for the flipping of protons through graphene with the assumption that they are initially chemisorbed at a high local coverage. Using DFT calculations, we found that the involved barriers notably reduce -with respect to the case of a unique chemisorbed proton (3.4 eV)- to about 1 eV when neighboring protons are adsorbed to the same carbon ring. For two protons chemisorbed to two adjacent carbon atoms in the ring (ortho dimer), the flipping mechanism[19] involves the insertion of one proton into the middle of the C-C bond, a bond that is restored after the process is completed. Rehybridization of these carbon

atoms at the transition state is at the origin of the reduction of the permeation barrier, as well as the increasing saturation of the carbon ring with chemisorbed protons, a feature that enlarges the ring area for the initial state[18]. In a related study, Feng *et al*[10] also found that hydrogenation of graphene greatly facilitates the permeation process.

Very recently, experiments by Sun *et al*[20] have shown that even hydrogen, as a gas (H_2), permeates pristine graphene with an activation energy close to that previously found for protons. Sun *et al* fabricated micrometre-size monocrystalline containers tightly sealed with graphene and, upon exposure to a gas atmosphere, they measured the eventual elevation of the membrane due to permeation of the gas inside the container. In stark contrast with measurements using other gases like He, they found a noticeable permeation of H_2 through graphene, ruled by an activation energy of about 1 eV. In addition, substitution by deuterium led to an undetectable permeation of the heavier isotope, in line with the isotopic effect found for their ionic counterparts[21]. To rationalize these findings, the authors proposed that molecular hydrogen first dissociates at graphene ripples and, in a second step, the chemisorbed atoms flip to the other side but no detailed insight has been provided for the mechanism responsible for the latter step.

Strongly motivated by these novel experimental evidences, in this work we propose and elucidate a possible mechanism which accounts for the permeation of chemisorbed hydrogen atoms through graphene. The present study can also be significant for the development of new technologies for hydrogen isotopic separation[22] as well as for a deeper understanding of hydrogen intercalation, which has been evidenced in graphene/substrate interfaces[23–25]. Also, the reported results are closely linked to studies of hydrogenated graphene[26, 27], a very active research field with applications in electronics[28], magnetism[29], hydrogen storage[30] and astrochemistry[31].

Indeed, as a starting point here we consider an increasing number of hydrogen atoms chemisorbed along the rim of a given carbon ring, and transition states and energy barriers for the flipping of a hydrogen atom are determined as a function of the number of the adjacent H atoms. To this end, DFT calculations were carried out by using molecular and periodic prototypes of graphene and the competition of permeation with other relevant processes in hydrogenated graphene[32] such as diffusion, desorption and recombination are also analyzed in detail.

Finally, the effect of charge doping of the graphene support and of hydrogen substitution

by deuterium on the mechanism responsible for the hydrogen permeation is also studied and discussed.

The article is organized as follows. Computational methods are described in Section 2. Section 3 is devoted to the presentation and discussion of results. Finally, conclusions are given in Section 4. Some auxiliary results are reported in a Supporting Material document.

2. COMPUTATIONAL METHODS

DFT calculations have been performed for the optimization of the hydrogenated circumcoronene ($C_{54}H_{18}$) and circumcircumcoronene ($C_{96}H_{24}$) structures by using the PBE[33] functional together with the 6-311+G[34] and cc-pVTZ[35] basis sets; moreover, the density fitting method[36] has been applied to approximate the two-electron repulsion integrals. In particular, the geometry optimization have been carried out at the PBE/6-311+G level and once the stationary points have been found the corresponding energy has been evaluated at the PBE/cc-pVTZ level by performing single point calculations. The correct nature of the obtained stationary points has been verified by carrying out harmonic frequency calculations, used in turn to estimate zero-point energy (ZPE) and thermal corrections (at 298 K and 1 atm) to the estimated thermodynamic properties, namely activation and reaction enthalpies. Intrinsic reaction coordinate calculations have been employed to check that reactants and products are indeed connected with the corresponding transition states for most of the investigated cases. In order to check the reliability of the obtained results, additional calculations have been performed by using both B3LYP[37] and M062X[38] functionals to carry out estimations for the relevant thermodynamic properties for a couple of cases related to the circumcoronene finite model. These estimations are reported in Table S1 of the Supporting Material where they are compared with those carried out by using the PBE functional. In there it can be appreciated that both absolute value and related trend of the PBE results are similar to those obtained with the B3LYP and M062X functionals, even if the latter provides in general more activated and more exothermic processes. All DFT computations have been performed by using the Gaussian 09 code[39].

In order to validate the results obtained for atomic hydrogen chemisorption by exploiting the finite model (based on $C_{54}H_{18}$ and $C_{96}H_{24}$), additional DFT calculations involving a periodic model of graphene have been carried out by using the same PBE functional as

implemented in the VASP code[40]: the projector augmented wave (PAW) method [41, 42] has been used with a cutoff energy of 600 eV for the plane-wave basis set and the Brillouin Zone was sampled by means of a 6×8×1 Monkhorst-Pack mesh[43]. Such a large number of k-points has been chosen in order to improve the accuracy of the results: it is well known indeed that graphene electronic properties calculations require particular care in the sampling of the Brillouin zone to reach the convergence[44]. The pristine supercell sheet of graphene, constituted by 216 C atoms, has been built independently and not based on the features of the finite prototypes. To do that, a basic tetragonal (4-atoms) cell instead of the conventional hexagonal one has been used [45–47]. All atoms of the supercell have been fully optimized (ions and lattice parameters) till forces were < 0.01 eV/Å. The so optimized graphene layer is characterized by in-plane lattice parameters a=25.64 Å and b=22.20 Å. Such parameters have been kept fixed in the estimation of the reported hydrogen adsorption energies, while a sufficiently thick amount of vacuum ($\sim$ 20 Å) has been added along the non-periodic direction in order to avoid any possible spurious interaction among replicas. Also, to check the reliability of these results, we have also considered a smaller supercell (180 C atoms, optimized lateral parameters a=21.37 Å and b=22.20 Å) and calculated the energy variation for the single hydrogenation process, which is found to differ by only $\sim$0.03 eV with respect to that for the larger cell.

3. RESULTS AND DISCUSSION

3.1. Chemisorption of H atoms

First, we address the question of graphene affinity for the chemical adsorption of hydrogen atoms. To this aim two different molecular graphene prototypes (circumcoronene and circumcircumcoronene) as well as a periodic model are considered and the sequential sticking of hydrogen atoms above the same carbon ring is studied. In particular, in the upper panel of Fig. 1, we report the electronic energy variation (ΔE) as a function of the number n of chemisorbed hydrogen atoms (H), which corresponds to the gas phase process

$$C_xH_y + nH \rightarrow (C_xH_{y+n}), \tag{1}$$

where C_xH_y represents the unsaturated (n=0) graphene prototype. In the lower panel of
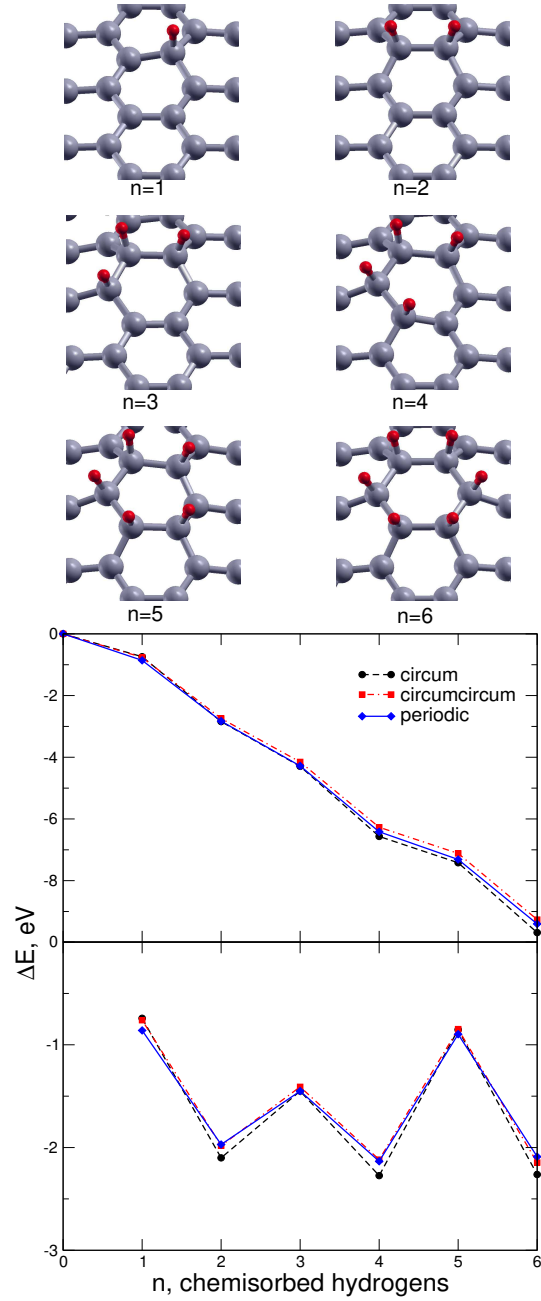
FIG. 1. Sequential hydrogenation of a graphenic single ring. Upper panel: electronic energy variation (ΔE) corresponding to the addition of n hydrogen atoms, with respect to the unsaturated graphene molecular prototype (n=0) and n isolated hydrogen atoms (see Eq. 1). Lower panel: electronic energy variation (ΔE) at each hydrogenation step (($n-1$)→(n), n=1-6 (see Eq. 2)). Black circles and red squares correspond to circumcoronene ($C_{54}H_{18}$) and circumcircumcoronene ($C_{96}H_{24}$) molecular prototypes, respectively, while blue diamonds to a periodic model of the graphenic plane.

Fig. 1 we depict instead the electronic energy variation at each hydrogenation step, which is defined as the ΔE of the following process

$$(C_xH_{y+n-1}) + H \rightarrow (C_xH_{y+n}), \; n = 1 - 6. \tag{2}$$
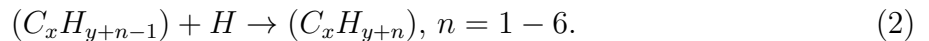
First of all, it can be appreciated that the obtained results do not significantly depend on the size of the employed graphene molecular prototypes since they provide energy variations that are close to each other. Moreover, the estimations carried out with both finite models are consistent with those for the periodic model which indeed serve as a validation test of the former. This suggests that both circumcoronene and circumcircumcoronene can be safely used to obtain reliable estimations related to atomic hydrogen chemisorption and in the following Figures and Tables all reported results refer to the graphene finite prototypes.

More in details, it can be seen that in all cases the consecutive addition of hydrogen atoms to the same ring is an energetically favourable process (negative ΔE for every n): in fact, except for the sticking of the first and fifth hydrogen for which ΔE is about -0.8 eV, the electronic variation is larger (in absolute value) than -1.0 eV. In particular, the most favourable values are found for even n for which $\Delta E \simeq$ -2.0 eV. A simple explanation for the observed oscillations in the energy variation can be given considering the closed-shell or open-shell nature of the given species to which hydrogen is added. For an even n product in Eq. 2 - and for the considered arrangements of H atoms - we expect a stable closed-shell system whereas the associated reactant is an open-shell reactive species both leading to a large energy variation. Conversely, for odd n we expect an open-shell product whereas the reactant was a stable closed-shell species both leading to a smaller energy variation. Further support to this argument will be given below when discussing the features of the sticking barrier. A complementary interpretation can be given considering the periodic nature of graphene since the behaviour observed in Fig.1 reflects the presence in the honeycomb plane of two different sublattices. In fact, for even n the hydrogen atoms equally occupy both sublattices leading to a particularly stable arrangement of chemisorbed atoms, as already shown in the case of hydrogen dimers[29], due to a nonmagnetic coupling with total spin S=0. For odd n, the two sublattices are inevitably not equally occupied leaving one electron deriving from one broken π bond unpaired: this leads to a lower energy variation for the hydrogen addition since it represents a less stable configuration with respect to the cases with even n, all characterized by paired electrons. Therefore, present results demonstrate

TABLE I. Hydrogen sticking barriers obtained as the electronic energy and enthalpy variation for each hydrogenation step (see Eq. 2 and Fig. 1). Values are in eV.

	n=1	n=2	n=3	n=4	n=5	n=6
ΔE	0.23	0	0.16	0	0.24	0
ΔH	0.24	0	0.16	0	0.27	0

that the saturation of a single graphenic ring with hydrogen atoms is energetically possible in the gas phase.

At this point it is useful to stress that the related hydrogen sticking barrier is low and in general theoretical estimations[32] provide values falling between 0.2 and 0.4 eV. Recently, an experimental measurement of the hydrogen chemisorption threshold has been also obtained[48], providing a value ($\sim$ 0.4 eV) in agreement with the theoretical estimations. Our prediction (considering the zero-point energy and thermal corrections) of the involved barrier is 0.24 eV (see Table I), which is in agreement with recent calculations obtained at a similar level of theory (See Supporting Material of Ref.[48]). However, the latter estimation is likely be underestimated as found from the comparison with the corresponding CCSD(T) computation (giving 0.37 eV[49]) of H addition to coronene. We have checked, as reported in Table I, that at each of the hydrogenation steps here considered the sticking barrier does not significantly vary for odd n, while we have been unable to find any barrier for even n. The latter is consistent with the results reported in Ref.[50] for the chemisorption of two H atoms at low temperatures: in particular in there the authors showed that for the adsorption of a second H atom the sticking barrier significantly lowers or disappears. Furthermore, the observed behavior is consistent with the closed-shell vs open-shell character explanation given above. For even n product the reaction involves the addition of two radicals, a process which is expected to be barrierless, whereas for odd n product it involves a closed-shell reactant species and the reaction has to disrupt its delocalized electron pattern, associated with a greater stability, in order to form a radical product.

Present predictions showing that a high local density of hydrogen H is both thermodinamically and kinetically favourable seem apparently to be incompatible with the maximum experimental coverage (hydrogen/carbon ratio), which is believed to be below 40%[51, 52] for atomic H and deuterium adsorbed on extended graphene. However, it must be pointed

TABLE II. Electronic energy and enthalphy variations associated to the most favorable single hydrogen flipping process for an increasing number (n) of chemisorbed hydrogens on a graphenic carbon ring. The reported energy balances between reactants (R) and transition state (TS) (as well as products (P)) correspond to the results obtained exploiting the finite (based on circumcoronene and circumcircumcoronene) model. All values are in eV.

| chemisorbed | R→TS | | | | R→P | | | |
| | ΔE_a | | ΔH_a | | ΔE_r | | ΔH_r | |
hydrogens	circum	circumcircum	circum	circumcircum	circum	circumcircum	circum	circumcircum
n=1	4.36	4.41	4.16	4.26	0.00	0.00	0.0	0.0
n=2	2.86	2.92	2.71	2.84	-0.45	-0.49	-0.45	-0.55
n=3	2.58	2.68	2.45	2.59	-0.48	-0.53	-0.51	-0.56
n=4	2.79	2.58	2.67	2.49	-0.51	-0.55	-0.50	-0.56
n=5	1.70	1.73	1.58	1.65	-0.71	-0.76	-0.73	-0.78
n=6	2.98	2.84	2.79	2.69	-1.59	-1.73	-1.64	-1.77

out that the detected experimental coverage is in general not uniform[24] over the graphene surface with both clean and high H density areas. In those areas with high coverage not only H adatom dimers[50] are found but also more complex structures due to H clustering[53], which has been shown to specially occur in curved regions and protrusions of the surface. Therefore, although the full hydrogenation of extended graphene samples has been not experimentally achieved yet as for the case of finite carbon platforms such as coronene[54], we consider that regions with a high density of H adatoms should locally exist on 2D carbon layers (see also a discussion on the topic in Section 3.3 of Ref.[32].

3.2. Hydrogen permeation and competing processes

Having established the features of graphenic single ring being progressively saturated by H adatoms, we start studying the hydrogen permeation through the same flipping mechanism we have previously found[18] in the case of protons. In this mechanism (see upper part of Fig. 2) the hydrogen atom can pass through the middle of the C-C bond connecting to the closest chemisorbed additional hydrogen ("insertion" transition state) and flips to the other side of the carbon plane. Note that the flipping hydrogen is that located at one end of the row
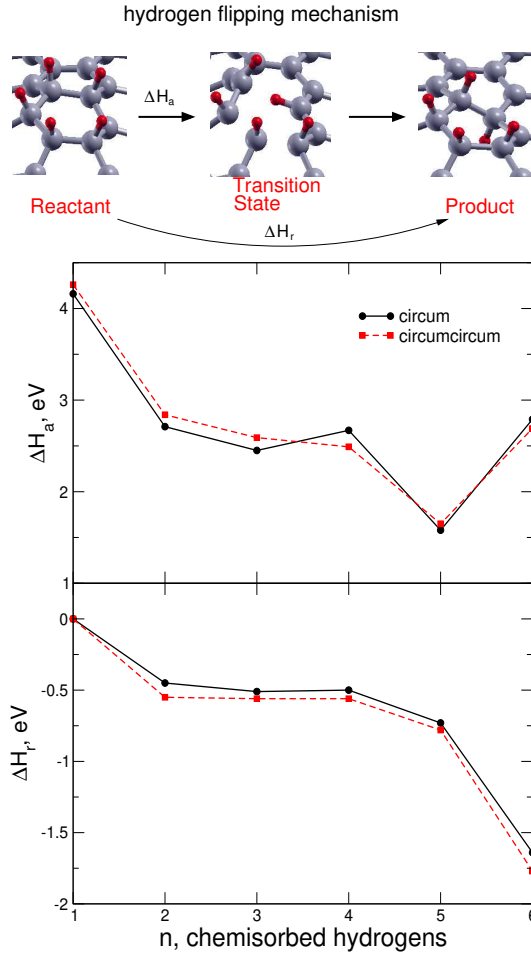
FIG. 2. Activation (ΔH_a) and reaction (ΔH_r) enthalpies for the permeation, via an insertion mechanism, of a hydrogen atom through graphene as a function of the number of consecutive chemisorbed hydrogens along the same carbon ring. Black circles and red squares correspond to circumcoronene and circumcircumcoronene graphene molecular prototypes, respectively. In the upper part the main features of the insertion mechanism (for the specific case of $n=5$) are sketched: the sp^2-like character of the carbon atoms pertaining to the breaking C-C bond can be noticed in the transition state.

of n chemisorbed atoms. For this insertion process to occur, the C-C bond effectively breaks but the C-H bond remains preserved. It must be also stressed that in the related transition state (TS) both carbon atoms pertaining to the breaking C-C bond have practically lost their initial sp^3 hybridization character and rather show sp^2-like configurations with two planar carbon rings that are almost perpendicular to each other (see upper part of Fig. 2). This leads to a related activation energy (and enthalpy) which tends to decrease with the

number of chemisorbed atoms, n, as shown in Table II and in the upper panel of Fig. 2.

As for the corresponding reaction enthalpy, it is always negative, except for n=1, and its absolute value increases with n as seen in Table II and in the lower panel of Fig. 2. In particular, even if the activation energy is larger than 4.0 eV for n=1, it drops to less than 3.0 eV for n=2 and then decreases down to a minimum of about 1.6-1.7 eV for n=5; the reaction energy, in turn, appears to be almost constant and equal to -0.5 eV for n=2-4 and drops down to about -1.7 eV for n=6, in a similar way as already shown in the case of protons (see Table 1 of Ref.[18]). This therefore confirms that this flipping process is always exothermic for n >1 and becomes more favourable when the graphenic ring reaches the complete saturation. In general, it can be also appreciated that present values are slightly more exothermic (up to 0.4 eV for the highest n) than those obtained in the case of proton permeation (see Table 1 of Ref.[18]).

It must be stressed that the results in Fig. 2 obtained for circumcoronene and circumcircumcoronene are consistent and well agree to each other, confirming that both finite models for the graphene support are reliable. Therefore, for the sake of simplicity, in the following the reported results are those obtained by using the circumcoronene model.

At this is point, it is worth to consider those processes which can be competitive with that of the hydrogen insertion. Indeed, chemisorbed hydrogens can also undergo diffusion, desorption and recombination processes[32]. In fact, a sticked hydrogen could migrate to an adjacent carbon atom of the same ring; it could undergo desorption through a dehydrogenation step, the inverse process of that in Eq. 2; it could also recombine with a neighbour hydrogen atom to form one H_2 molecule, which desorbs far away. Further competitive processes, such as hydrogen migration from its chemisorption site to the nearest neighbour in the same sublattice, which is expected with a similar activation as direct diffusion, have been not taken into account for the sake of simplicity.

The enthalpy balances related to the considered possible outcomes for the outer chemisorbed hydrogen atom on a given graphenic ring are reported in Table III as a function of n together with sketches that schematically illustrate the involved processes. Notice that, for even n and in the case of desorption, ΔH_a assumes the same value as ΔH_r since for this process no transition state can be found.

The first thing to be stressed is that the hydrogen flipping through an insertion process is the only one being exothermic for all n=2-6. In fact, for both diffusion and desorption

ΔH_r is always positive (except $n=5$ for diffusion being reactant and product degenerate configurations) while recombination is the most exothermic one for $n=2$-5 but becomes endothermic for n=6. As for the activation enthalpy, it is clear that at all n the flipping process is that having the largest ΔH_a especially for the lower n and therefore it is expected to be globally less frequent. However, for larger n the differences between the related ΔH_a tend to reduce, especially for $n=5$. For this specific configuration the most probable event would be desorption ($\Delta H_a=0.90$ eV) but the product would be less stable than the reactant and the desorbed hydrogen could stick back due to a low energy barrier (see Table I); hydrogen diffusion would almost equally occur ($\Delta H_a=1.06$ eV) but it could lead to an analogous (and degenerate) configuration as that for the reactant. Also for $n=5$, ΔH_a for the flipping process is in turn larger than those of desorption and diffusion by 0.5-0.7 eV but for the hydrogen flipped on the other side it would be less probable to flip back being the related activation enthalpy around 2.2 eV. Similar considerations could stand for the $n=6$, considering also that in this case ΔH_r is the most negative for the flipping.

As for the recombination process, the obtained ΔH_a and ΔH_r for $n=2$ are in agreement with the theoretical estimations at a similar DFT level reported in Ref.[55]; for larger n we have reported the values related to the most favourable ("ortho" or "para") recombination mechanism and it can be seen that the related activation enthalphies are in general larger than those of the competing processes.

Therefore, this analysis suggests that at high coverage the hydrogen flipping through the insertion mechanism, even if not the most probable, it could occur and it would lead to the most favourable outcome (i.e. for $n=6$).

However, the lowest estimations for the activation enthalpy related to the flipping process we have obtained so far are still somewhat high if compared with that of about 1.0 eV recently reported[20] for the permeation of hydrogen through defect-free graphene. Thus, we have also considered alternative arrangements of a minimum number of chemisorbed atoms which could lead to a lower permeation barrier. Particularly interesting is the $n=2+2$ arrangement, with two nonconsecutive couples of hydrogen atoms chemisorbed on the same graphenic ring, whose possible formation path is shown in Fig. S1 of the Supporting Material together with that of the standard $n=4$ arrangement: in there it is shown that the $n=2+2$ arrangement is energetically favourable both globally and at each hydrogenation step, even if less stable than the previous $n=4$ case. For this arrangement it exists indeed a more
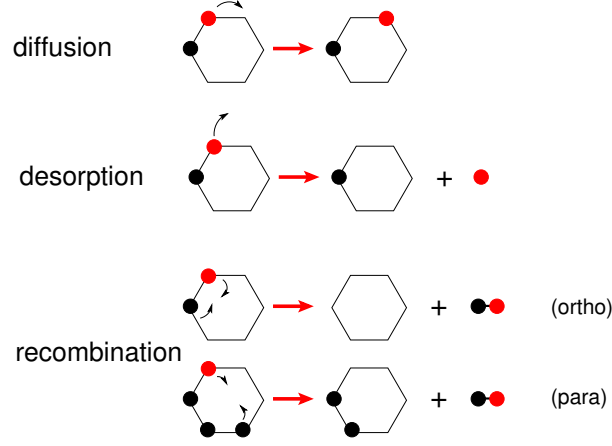
TABLE III. Activation and reaction energy for the hydrogen flipping, diffusion, desorption and recombination processes obtained as the corresponding enthalpy variations, ΔH_a and ΔH_r, respectively. The diffusion, desorption and recombination processes are sketched above for a minimum number of couples of adjacent chemisorbed atoms. Hydrogen diffusion corresponds to the migration of the outer chemisorbed H atom to the contiguous carbon atom of the same ring (or adjacent ring for $n=6$). Hydrogen desorption corresponds to the dehydrogenation step, the inverse process of that in Eq. 2. Hydrogen recombination corresponds to the simultaneous desorption of two H atoms to form one H_2 molecule through an ortho or para mechanism (see sketch above). Values are in eV.

flipping	n=2	n=3	n=4	n=5	n=6
ΔH_a	2.71	2.45	2.67	1.58	2.79
ΔH_r	-0.45	-0.51	-0.50	-0.73	-1.64
diffusion	n=2	n=3	n=4	n=5	n=6
ΔH_a	1.55	1.29	1.79	1.06	1.64
ΔH_r	1.40	0.36	1.78	0.00	1.65
desorption	n=2	n=3	n=4	n=5	n=6
ΔH_a	1.84	1.40	2.02	0.90	1.93
ΔH_r	1.84	1.23	2.02	0.63	1.93
recombination	n=2 [a]	n=3[a]	n=4 [b]	n=5[a]	n=6 [b]
ΔH_a	2.42	2.50	1.84	2.32	3.27
ΔH_r	-1.90	-1.24	-1.06	-1.66	0.09

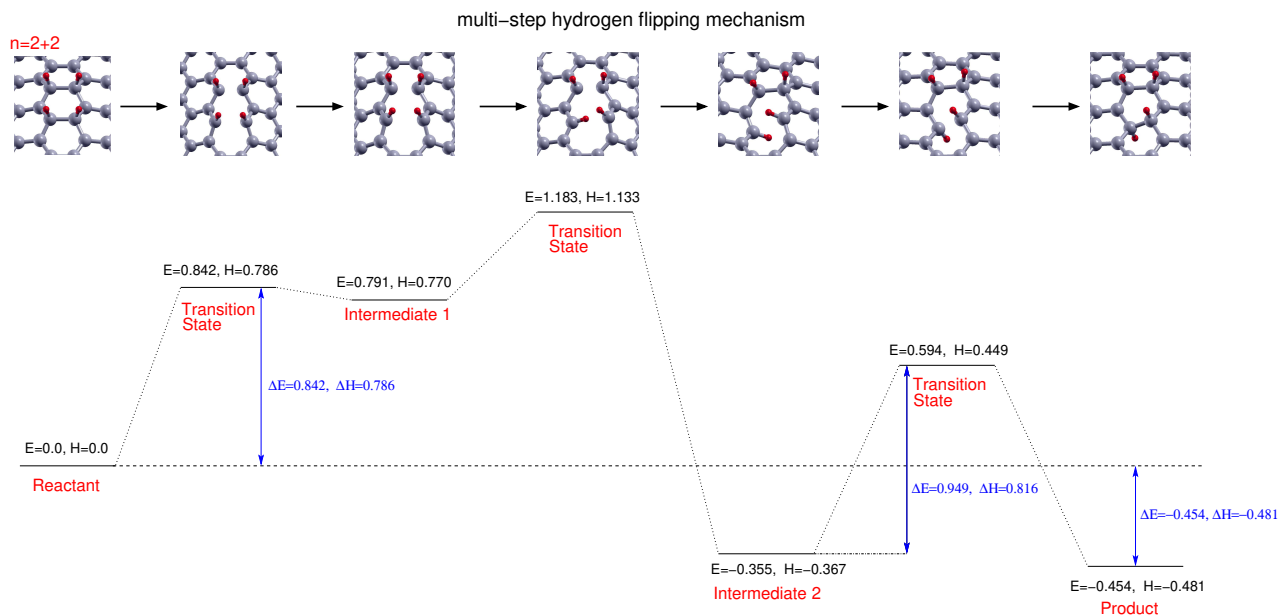[a] ortho recombination

[b] para recombination

FIG. 3. Multi-step hydrogen flipping mechanism starting from the $n=2+2$ arrangement. The electronic energy and enthalpy variation are evidenced for the most activated steps as well as for the global process.

elaborated mechanism which leads to the hydrogen flipping, as shown in Fig. 3. It goes through several steps which also involve two intermediate arrangements being the second one (Intermediate 2) particularly peculiar: it is characterized by both carbon atoms linked to the flipping and neighboring hydrogen atoms showing a clear sp^2 hybridization, as for the preceding transition state but with almost parallel planes, instead of perpendicular. This intermediate appears to be particularly stable and it is connected to the final product, where the sp^3 hybridization is recovered, by the most activated step showing an activation energy and enthalpy slightly below 1.0 eV.

It is worth pointing out that the C-C distance in the $n=2+2$ reactant configuration is about 1.62 Å, which is larger than those of the previously considered arrangements and globally contributing to a less activated hydrogen insertion.

In fact, in previous works devoted to the permeation of protons[10, 18] it has been argued that the enlargement of the carbon ring area in the initial state (reactant) is responsible for the decrease of the activation barrier as protons are succesively chemisorbed to the ring. In the present case, an increase of strain within and around that ring is also expected due to the formation of C-C single bonds and augmented H-H steric repulsion as more atoms

are chemisorbed. In particular, permeation should be facilitated if the C-C bond that is breaking at the transition state is already stretched in the reactant state. In Fig. S2 of the Supporting Material we depict the activation enthalpy as a function of the length of this C-C bond in the initial state for the various cases. As expected, this distance increases with the number of chemisorbed H atoms in the carbon ring (n=2-6) and becomes very large for the 2+2 chemisorption state. However, the activation enthalphy does not always decrease with the C-C distance, as occurred for the case of protons[18]. While the enthalpy certainly lowers along the sequence n= 3, 5 and 2+2, for n= 2, 4, and 6 it keeps high values irrespective of the elongation of the corresponding C-C bond. The latter feature must be due to the special stability of the n=even initial states, as discussed in the previous section (see also lower panel in Fig. 1). Therefore, besides the elongation of the involved bonds in the reactant state, relative destabilization of the latter (due to unpairing of electrons, for instance) is also contributing to the lowering of these permeation barriers.

In order to assess the viability of the multi-step mechanism illustrated in Fig. 3, in Table IV we also report the enthalpy balances for all possible processes originating from the n=2+2 arrangement: it can be seen that flipping is the process having in general the lowest activation enthalpy as well as a still negative reaction enthalpy. Indeed, for desorption we have reported for ΔH_a the same value as for ΔH_r since for this process no transition state has been obtained, as already pointed out above for the sticking barrier in the case of even n (see also Table I); therefore, if a hydrogen atom would tend to separate from the carbon plane towards desorption it could probably stick back. As for recombination, it can be seen that the formation of a H_2 molecule via an ortho mechanism is clearly more exothermic than insertion but the corresponding activation enthalpy is about 0.5 eV larger and therefore it is expected to be globally less frequent. Thus, in the case of the n=2+2 arrangement we have found that the insertion outcome is in principle the most probable and the corresponding activation enthalpy (ΔH_a=0.82 eV) is in good agreement with the recent experimental estimation (1.0 ±0.1 eV[20]).

3.3. Charge doping effects

At this point it is worth noting that the corresponding permeation activation energies for protons, reported in Table 1 of Ref.[18], are in general lower than those for hydrogens (see

TABLE IV. Activation and reaction enthalpy for the hydrogen flipping, diffusion, desorption and recombination processes which can occur starting from the $n=2+2$ arrangement (see also Fig.3). The reported ΔH_a for flipping corresponds to that of the limiting step, while for recombination ΔH_a and ΔH_r refer to the ortho mechanism (see also Table III). All values are in eV.

n=2+2	flipping	diff.	desorpt.	recomb.
ΔH_a	0.82	1.06	0.80	1.30
ΔH_r	-0.48	0.47	0.80	-3.00

Table II). This is particularly evident for $n=4, 6$ where lower values of about 1.0 eV are found in the case of protons. Therefore one may wonder whether this feature would depend on the global charge bore by the investigated system. Indeed, it has been theoretically predicted[56, 57] that charge doping can actually improve the adsorption energy as well as the mobility of hydrogen atoms chemisorbed on graphene. Therefore, to investigate this effect we have considered three different charge values on the circumcoronene substrate, namely -2, 0 and +2 a.u., corresponding to electron doping, no doping and hole doping, respectively, and the related results are reported in Fig. 4. In particular, in the upper panel we report the formation enthalpy (ΔH_f) of the hydrogenated carbon support with respect to the isolated support and n hydrogen atoms (see Eq. 1, with both non-hydrogenated and hydrogenated substrate bearing the charge doping). In the intermediate and lower panels of Fig. 4 we show related activation (ΔH_a) and reaction (ΔH_r) enthalpies, respectively.

In the upper panel, it can be seen that ΔH_f has an almost linear behaviour with respect to n for both doped results, with a more pronounced slope in the case of hole doping. This leads to more favourable formation enthalpies for hole doping at every n with respect to undoped results, which is particularly evident for $n=5$ (about 1.0 eV larger). A similar behaviour was found[58] in the case of di-hydrogenated (two hydrogen adatoms) graphene with hole doping leading to larger binding energies with respect to electron doping. In our calculation of the charge doped isolated circumcoronene it was found that, in both cases (charge +2 and -2 a.u.), there exists a triplet state which is quasi-degenerate with the lowest singlet state. Thus, when interacting with the added hydrogen atoms (odd values of n), the doped substrate now can easily acquire an open-shell character (that of the low-lying triplet state) which explains the larger formation enthalpies compared with the neutral

case where the substrate is a very stable closed-shell structure. In the case of even n, the effect is less pronounced since the neutral substrate also has an open-shell character and in this case the overall positive charge in the hole-doped substrate also plays an important role. Furthermore, notice in the upper panel of Fig. 4 that the doped curves have lost the oscillations with respect to n observed in the neutral case, which is again consistent with the open-shell character of the doped reactants for all values of n.

More interestingly, both electron and hole doping provide a reduction of ΔH_a, which is particularly significant for $n=4$, 6, as seen in the intermediate panel. As a result, for $n > 3$ the activation enthalpy ranges around 1.5 eV for both dopings, mimicking the behaviour reported for protons in Table 1 and Fig. 4 of Ref.[18], with electron doping in general leading to slightly lower values. In the case of the electron doping, we have checked for $n=4$ that the TS is characterized by an extra stabilization with respect to the reactant due to the larger affinity of the former. This is confirmed by a charge distribution analysis[59] (see Table S2 in the Supporting Material) which has shown that those carbon atoms of the TS supporting the chemisorbed hydrogen atoms and characterized by the sp^2 hybridization are indeed bearing a larger fraction of the negative charge with respect to the sp^3 hydridized neighboring atoms (as well as compared with their counterparts on the reactant species). As for the hole doping, both reactant and TS species are about 14-15 eV less stable than the corresponding neutral counterparts due to the high ionization energy of the latter. However, we have found (i.e. for $n=4$) a lower ionization energy in the case of the neutral TS of about 1.0 eV with respect to that of the neutral reactant and this can be due to its higher capacity of charge delocalization, as found by a larger partial positive charge globally bore by both the chemisorbed hydrogen and related supporting carbon atoms (see Table S2).

On what concerns the effect on ΔH_r, in the lower panel it can be noted that while electron doping is in general slightly more exothermic, the opposite can be observed for hole doping. These results suggest that charge doping can help to reduce the barrier associated to the hydrogen flipping mechanism: in general, electron doping leads to slightly more favourable values for both activation and reaction enthalpies. In addition, we have checked that in the case of the electron doping, even if the activation enthalpy is also diminished for the diffusion and desorption processes, this reduction is less relevant and put the related barriers in the same range (around 1.4-1.7 eV) as for the flipping processes (see the results in Table S3 of the Supporting Material obtained for the $n=4$ arrangement). This does not occur

in the case of hole doping since this leads to a more significant decrease of the activation enthalpy (down to 0.9 eV) for the diffusion outcome which clearly becomes the most likely process (see Table S3). Therefore, we can conclude that when a given graphenic ring is highly saturated with hydrogens the possibility of their permeation is not negligible and can be facilitated by electron doping.

Further studies on charge doping effects by exploiting periodic models would help to complement present results since they allow to get rid of border effects in the charge distribution which are unavoidable in the molecular finite prototypes. Moreover, a periodic model (or a quite larger molecular prototype) would also facilitate to obtain charge densities closer to those attained experimentally (our simulations correspond to a charge density of about $\pm 10^{14}$ a.u./cm^2 whereas experiments using gate voltage[60] provide much lower densities, around 2×10^{12} a.u./cm^2).

3.4. Isotopic effects

Since the reported activation and reaction enthalpies include ZPE contributions it is also possible to evaluate the corresponding thermodynamic properties for deuterium (D) chemisorbed atoms. To do that we have first considered the flipping of one deuterium atom for the n=4,5 cases (as in Fig.1 but with chemisorbed deuterium atoms) and calculated the ΔH_a and ΔH_r enthalpy balances, which are compared with those for the non-deuterated counterparts, as shown in Table S4 of the Supporting Material. In there it can be seen that for both activation and reaction enthalpies the flipping of one hydrogen atom is slightly favoured by just a few meV with respect to that of one deuterium atom. This small deviation is a consequence of the fact that ZPE corrections are important not only for the reactant but also for the transition and product states which provide comparable ZPE values, being their hydrogen/deuterium difference around 90 meV per chemisorbed atom, in agreement with previous determinations[51].

The obtained small differences demonstrate an almost negligible isotopic effect for the flipping process and they are certainly not sufficient to explain that deuterium permeation is not experimentally discerned in Ref.[20] within the considered detection limit. However, in addition to the flipping, we believe that other processes should be taken into account such as molecular hydrogen(deuterium) recombination. In fact, once at least two H(D) atoms
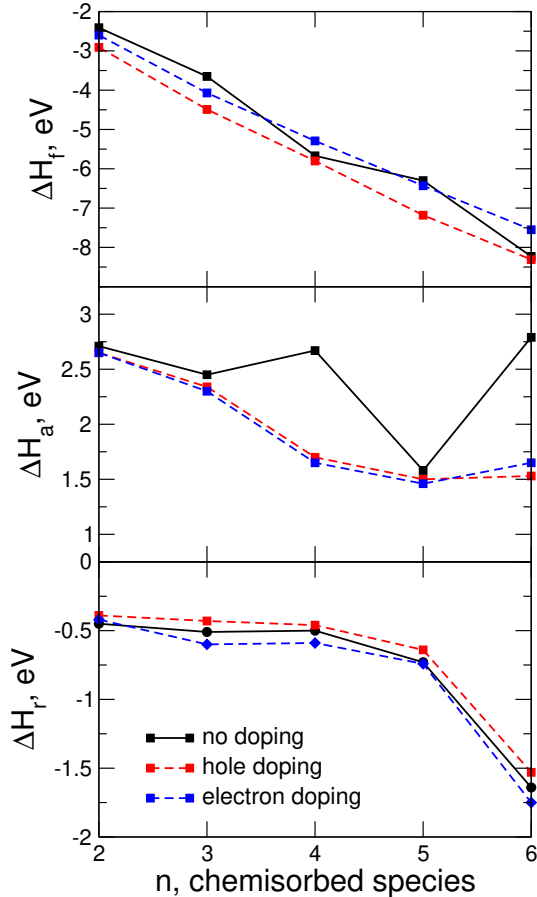
FIG. 4. Upper panel: electron (total charge q=-2 a.u.) and hole (q=2 a.u.) doping effect on the formation enthalpy (ΔH_f) for the sequential addition of hydrogen on a graphenic ring. Intermediate panel: charge doping effect on the activation enthalpy (ΔH_a) for the hydrogen permeation via a flipping mechanism. Lower panel: charge doping effect on the reaction enthalpy (ΔH_r) for the hydrogen permeation via a flipping mechanism. Note that the "no doping" results are those already shown in Figs. 1 and 2 and are here reported for the sake of comparison.

found themselves on the other side of the graphene membrane they should react to form $H_2(D_2)$ in order to increase the container gas pressure which is responsible for the lifting of the membrane itself. Therefore, ZPE effects have been also considered for the recombination paths starting from the n=2 arrangements and through the para and ortho mechanisms (see Table III), which lead to $H_2(D_2)$ formation, and the related estimations are also reported in Table S4. In there it can be seen that H_2 formation is less activated than that of D_2 by about 65-100 meV and that the lighter isotope leads to a larger exothermic process of about 90-100 meV. We consider that the computed ΔH_a and ΔH_r estimations, which

evidence non negligible differences for the recombination related to two isotopic species, clearly indicate that the permeation of the lighter species is globally favoured both kinetically and thermodynamically. We believe that present predictions on graphene isotopic selectivity are qualitatively compatible with the experimental findings of Ref.[20]. Moreover, additional quantum effects such as tunneling, here not considered for the sake of simplicity, are also expected to further facilitate[13] hydrogen transmission with respect to deuterium, therefore providing an additional support to the experimental evidences.

4. SUMMARY AND OUTLOOK

By means of DFT computations we have elucidated a cooperative mechanism leading to the flipping of a chemisorbed atomic hydrogen from one side to the other of a graphene layer. We have demonstrated that the effectiveness of this mechanism, which involves a rearrangement of the orbital hybridization of the participant carbon atoms and the insertion of the flipping species between them, is highly dependent on the local density of the chemisorbed hydrogen atoms on the 2D carbon surface. In particular, for a low saturation of a given graphenic ring the transmission of atomic hydrogen is highly unlikely since alternative outcomes such as diffusion and desorption exhibit quite lower activation enthalpies. However, when a graphenic ring tends to saturation, the proposed flipping mechanism becomes competitive leading to a significant exothermic process. Moreover, we have shown that there exists at least one specific configuration of few neighboring chemisorbed hydrogen atoms for which the flipping of one hydrogen becomes the most likely process with a related limiting activation enthalpy which is in the range of the recent experimental estimation[20] of the barrier for hydrogen transmission through defect-free graphene. Present results provide solid support to a flipping mechanism responsible for the hydrogen transmission through pristine graphene and also suggest that electron doping could help to improve its performance. We also consider that the proposed mechanism can be useful to provide a deeper understanding of atomic hydrogen intercalation which has been experimentally observed[24, 25] in hydrogenated graphene/substrate interfaces. Additionally, ZPE effects have been also considered and they suggest that the trasmission of H_2 is favoured over D_2 both kinetically and thermodynamically. In order to fully assess the role of quantum effects on hydrogen trasmission in the near future we plan to investigate the impact of tunneling on the involved processes.

We also believe that a detailed investigation of the effect of the membrane curvature on the computed magnitudes is also highly desirable and deserves to be addressed.

ACKNOWLEDGMENTS

SUPPORTING MATERIAL

Additional tables with: B3LYP and M062X estimations of the magnitudes of interest for the $n=4,5$ cases; partial charge values for the doped and undoped circumcoronene prototype related to $n=4$ case; the doping dependence of the competitive processes originating from the $n=4$ arrangement; the isotopic dependence of the activation and reaction enthalpies for the flipping and recombination processes. Additional figures showing a comparison between possible hydrogenation paths for the $n=2+2$ and $n=4$ arrangements as well as bond length dependence of the activation enthalpy for flipping. This material is available free of charge via the Internet.

[1] L. Wang, M.S.H. Boutilier, P.R. Kidambi, D. Jang, N.G. Hadjiconstantinou, and R. Karnik, "Fundamental transport mechanisms, fabrication and potential applications of nanoporous atomically thin membranes," Nature Nanotechnology. **12**, 509–522 (2017).

[2] J.S. Bunch, S.S. Verbridge, J.S. Alden, A.M. van der Zande, J.M. Parpia, H.G. Craighead, and P.L. McEuen, "Impermeable atomic membranes from graphene sheets," Nano Letters. **8**, 2458–2462 (2008).

[3] V. Berry, "Impermeability of graphene and its applications," Carbon **62**, 1–10 (2013).

[4] M. Miao, M. B. Nardelli, Q. Wang, and Y. Liu, "First principles study of the permeability of graphene to hydrogen atoms," Physical Chemistry Chemical Physics **15**, 16132–16137 (2013).

[5] S. Hu, M. Lozada-Hidalgo, F. C. Wang, A. Mishchenko, F. Schedin, R. R. Nair, E. W. Hill, D. W. Boukhvalov, M. I. Katsnelson, R. A. W. Dryfe, I. V. Grigorieva, H. A. Wu, and A. K. Geim, "Proton transport through one-atom-thick crystals," Nature **516**, 227–230 (2014).

[6] M. Seel and R. Pandey, "Proton and hydrogen transport through two-dimensional monolayers," 2D Materials **3**, 025004 (2016).

[7] J. M. H. Kroes, A. Fasolino, and M. I. Katsnelson, "Density functional based simulations of proton permeation of graphene and hexagonal boron nitride," Phys. Chem. Chem. Phys. **19**, 5813–5817 (2017).

[8] L. Shi, A. Xu, G. Chen, and T. Zhao, "Theoretical understanding of mechanisms of proton exchange membranes made of 2d crystals with ultrahigh selectivity," The Journal of Physical Chemistry Letters. **8**, 4354–4361 (2017).

[9] N. T. Ekanayake, J. Huang, J. Jakowski, B. G. Sumpter, and S. Garashchuk, "Relevance of the nuclear quantum effects on the proton/deuteron transmission through hexagonal boron nitride and graphene monolayers," Journal of Physical Chemistry C **121**, 24335–24344 (2017).

[10] Y. Feng, J. Chen, W. Fang, E.-G. Wang, A. Michaelides, and X.-Z. Li, "Hydrogenation facilitates proton transfer through two-dimensional honeycomb crystals," The Journal of Physical Chemistry Letters. **8**, 6009–6014 (2017).

[11] S. Bukola, Y. Liang, C. Korzeniewski, J. Harris, and S. Creager, "Selective proton/deuteron transport through nafion—graphene—nafion sandwich structures at high current density," Journal of the American Chemical Society **140**, 1743–1752 (2018).

[12] I. Poltavsky, L. Zheng, M. Mortazavi, and A. Tkatchenko, "Quantum Tunneling of Thermal Protons Through Pristine Graphene," Journal of Chemical Physics **148**, 204707 (2018).

[13] J. W. Mazzuca and N. K. Haut, "Theoretical Description of Quantum Mechanical Permeation of Graphene Membranes by Charged Hydrogen Isotopes," Journal of Chemical Physics **148**, 224301 (2018).

[14] W. Fu, Y. Wang, S. Hu, X. Zhou, and X. Long, "Hydrogen isotope separation via ion penetration through group-iv monolayer materials in electrochemical environment," The Journal of Physical Chemistry Letters **10**, 4618–4624 (2019).

[15] M. I. Walker, P. Braeuninger-Weimer, R. S. Weatherup, S. Hofmann, and U. F. Keyser, "Measuring the proton selectivity of graphene membranes," Applied Physics Letters **107**, 213104 (2015).

[16] J. L. Achtyl, R. R. Unocic, L. Xu, Y. Cai, M. Raju, W. Zhang, R. L. Sacci, I. V. Vlassiouk, P. F. Fulvio, P. Ganesh, D. J. Wesolowski, S. Dai, A. C. T. van Duin, M. Neurock, and F. M. Geiger, "Aqueous proton transfer across single-layer graphene," Nature Communications **6**, 6539 (2015).

[17] Y. An, A. F. Oliveira, T. Brumme, A. Kuc, and T. Heine, "Stone-wales defects cause high proton permeability and isotope selectivity of single-layer graphene," Advanced Materials **32**, 2002442 (2020).

[18] M. Bartolomei, M. I. Hernández, J. Campos-Martínez, and R. Hernández-Lamoneda, "Graphene multi-protonation: A cooperative mechanism for proton permeation," Carbon **144**, 724–730 (2019).

[19] S. M. Lee, K. H. An, G. Seifert, Y. H. Lee, and T. Frauenheim, "A hydrogen storage mechanism in single-walled carbon nanotubes," Journal of the American Chemical Society. **123**, 5059–5063 (2001).

[20] P. Z. Sun, Q. Yang, W. J. Kuang, Y. V. Stebunov, W. Q. Xiong, J. Yu, R. R. Nair, M. I. Katsnelson, S. J. Yuan, I. V. Grigorieva, M. Lozada-Hidalgo, F. C. Wang, and A. K. Geim, "Limits on gas impermeability of graphene," Nature **579**, 229–232 (2020).

[21] M. Lozada-Hidalgo, S. Hu, O. Marshall, A. Mishchenko, A. N. Grigorenko, R. A. W. Dryfe, B. Radha, I. V. Grigorieva, and A. K. Geim, "Sieving hydrogen isotopes through two-dimensional crystals," Science **351**, 68–70 (2016).

[22] M. Lozada-Hidalgo, S. Zhang, S. Hu, A. Esfandiar, I.V. Grigorieva, and A.K. Geim, "Scalable and efficient separation of hydrogen isotopes using graphene-based electrochemical pumping," Nature Communications. **8**, 15215 (2017).

[23] C. Riedl, C. Coletti, T. Iwasaki, A. A. Zakharov, and U. Starke, "Quasi-free-standing epitaxial graphene on sic obtained by hydrogen intercalation," Phys. Rev. Lett. **103**, 246804 (2009).

[24] C. Lin, Y. Feng, Y. Xiao, M. Drr, X. Huang, X. Xu, R. Zhao, E. Wang, X.-Z. Li, and Z. Hu, "Direct observation of ordered configurations of hydrogen adatoms on graphene," Nano Letters **15**, 903–908 (2015).

[25] D. Lizzit, M.I. Trioni, L. Bignardi, P. Lacovig, S. Lizzit, R. Martinazzo, and R. Larciprete, "Dual-route hydrogenation of the graphene/ni interface," ACS Nano **13**, 1828–1838 (2019), https://doi.org/10.1021/acsnano.8b07996.

[26] D. C. Elias, R. R. Nair, T. M. G. Mohiuddin, S. V. Morozov, P. Blake, M. P. Halsall, A. C. Ferrari, D. W. Boukhvalov, M. I. Katsnelson, A. K. Geim, and K. S. Novoselov, "Control of graphene's properties by reversible hydrogenation: Evidence for graphane," Science **323**, 610–613 (2009).

[27] K. E. Whitener, "Review article: Hydrogenated graphene: A users guide," Journal of Vacuum Science & Technology A **36**, 05G401 (2018), https://doi.org/10.1116/1.5034433.

[28] R. Balog, B. Jørgensen, L. Nilsson, M. Andersen, E. Rienks, M. Bianchi, M. Fanetti, E. Lægsgaard, A. Baraldi, S. Lizzit, Z. Sljivancanin, F. Besenbacher, B. Hammer, T. G. Pedersen, P. Hofmann, and L. Hornekær, "Bandgap opening in graphene induced by patterned hydrogen adsorption," Nature Materials **9**, 315–319 (2010).

[29] H. González-Herrero, J. M. Gómez-Rodríguez, P. Mallet, M. Moaied, J. J. Palacios, C. Salgado, M. M. Ugeda, J.-Y. Veuillen, F. Yndurain, and I. Brihuega, "Atomic-scale control of graphene magnetism by using hydrogen atoms," Science **352**, 437–441 (2016).

[30] K. S. Subrahmanyam, P. Kumar, U. Maitra, A. Govindaraj, K. P. S. S. Hembram, U. V. Waghmare, and C. N. R. Rao, "Chemical storage of hydrogen in few-layer graphene," Proceedings of the National Academy of Sciences **108**, 2674–2677 (2011), https://www.pnas.org/content/108/7/2674.full.pdf.

[31] G. Vidali, "H_2 formation on interestelar grains," Chem. Rev. **113**, 8762–8782 (2013).

[32] M. Bonfanti, S. Achilli, and R. Martinazzo, "Sticking of atomic hydrogen on graphene," Journal of Physics. Condensed Matter **30**, 283002 (2018).

[33] J.P. Perdew, K. Burke, and M. Ernzerhof, "Generalized gradient approximation made simple," Phys. Rev. Lett. **77**, 3865–3868 (1996).

[34] J. S. Binkley, J. A. Pople, and W. J. Hehre, "Self-consistent molecular orbital methods. 21. small split-valence basis sets for first-row elements," J. Am. Chem. Soc. **102**, 939–947 (1980).

[35] R. A. Kendall, T. H. Dunning, and R. J. Harrison, "Electron affinities of the first-row atoms revisited. systematic basis sets and wave functions," J. Chem. Phys. **96**, 6796–6806 (1992).

[36] O. Vahtras and J. Almöf an M.W. Feyereisen, "Integral approximations for lcao-scf calculations," Chem. Phys. Lett. **213**, 514–518 (1993).

[37] P. J. Stephens, F. J. Devlin, C. F. Chabalowski, and M. J. Frisch, "Ab initio calculation of vibrational absorption and circular dichroism spectra using density functional force fields," J. Phys. Chem. **98**, 11623–11627 (1994).

[38] Y. Zhao and D. G. Truhlar, "The m06 suite of density functionals for main group thermochemistry, thermochemical kinetics, noncovalent interactions, excited states, and transition elements: two new functionals and systematic testing of four m06-class functionals and 12 other functionals," Theoretical Chemistry Accounts **120**, 215–241 (2008).

[39] M. J. Frisch, G. W. Trucks, H. B. Schlegel, G. E. Scuseria, M. A. Robb, J. R. Cheeseman, G. Scalmani, V. Barone, B. Mennucci, G. A. Petersson, H. Nakatsuji, M. Caricato, X. Li, H. P. Hratchian, A. F. Izmaylov, J. Bloino, G. Zheng, J. L. Sonnenberg, M. Hada, M. Ehara, K. Toyota, R. Fukuda, J. Hasegawa, M. Ishida, T. Nakajima, Y. Honda, O. Kitao, H. Nakai, T. Vreven, J. A. Montgomery, Jr., J. E. Peralta, F. Ogliaro, M. Bearpark, J. J. Heyd, E. Brothers, K. N. Kudin, V. N. Staroverov, R. Kobayashi, J. Normand, K. Raghavachari, A. Rendell, J. C. Burant, S. S. Iyengar, J. Tomasi, M. Cossi, N. Rega, J. M. Millam, M. Klene, J. E. Knox, J. B. Cross, V. Bakken, C. Adamo, J. Jaramillo, R. Gomperts, R. E. Stratmann, O. Yazyev, A. J. Austin, R. Cammi, C. Pomelli, J. W. Ochterski, R. L. Martin, K. Morokuma, V. G. Zakrzewski, G. A. Voth, P. Salvador, J. J. Dannenberg, S. Dapprich, A. D. Daniels, Ö Farkas, J. B. Foresman, J. V. Ortiz, J. Cioslowski, and D. J. Fox, "Gaussian 09 Revision E.01," Gaussian Inc. Wallingford CT 2009.

[40] G. Kresse and J. Furthmüller, "Efficient iterative schemes for ab initio total-energy calculations using a plane-wave basis set," Phys. Rev. B **54**, 11169–11186 (1996).

[41] P.E. Blöchl, "Projector augmented-wave method," Phys. Rev. B **50**, 17953–17979 (1994).

[42] G. Kresse and D. Joubert, "From ultrasoft pseudopotentials to the projector augmented-wave method," Phys. Rev. B **59**, 1758–1775 (1999).

[43] H.J. Monkhorst and J.D. Pack, "Special points for brillouin-zone integrations," Phys. Rev. B **13**, 5188 (1976).

[44] S. Casolo, O.M. Løvvik, R. Martinazzo, and G.F. Tantardini, "Understanding adsorption of hydrogen atoms on graphene," J. Chem. Phys. **130**, 054704 (2009).

[45] L. Valentini, S. Bittolo Bon, and G. Giorgi, "Engineering graphene oxide/water interface from first principles to experiments for electrostatic protective composites," Polymers **12**, 1596 (2020).

[46] L. Valentini, S. Bittolo Bon, N.M. Pugno, M. Hernández Santana, M.A. López-Manchado, and G. Giorgi, "Synergistic icephobic behaviour of swollen nitrile butadiene rubber graphene and/or carbon nanotube composites," Compos. B: Eng **166**, 352–360 (2019).

[47] Y. Masuda, G. Giorgi, and K. Yamashita, "Dft study of anatase-derived tio$_2$ nanosheets/graphene hybrid materials," Phys. Status Solidi B **251**, 1471–1479 (2014).

[48] H. Jiang, M. Kammler, F. Ding, Y. Dorenkamp, F. R. Manby, A. M. Wodtke, T. F. Miller III, A. Kandratsenka, and Oliver Bünermann, "Imaging covalent bond formation by h atom scattering from graphene," Science **364**, 379–382 (2019).

[49] Y. Wang, H. J. Qian, K. Morokuma, and S. Irle, "Coupled cluster and density functional theory calculations of atomic hydrogen chemisorption on pyrene and coronene as model systems for graphene hydrogenation," The Journal of Physical Chemistry A. **116**, 7154–7160 (2012).

[50] H. González-Herrero, E. Cortés del Río, P. Mallet, J.-Y. Veuillen, J. J. Palacios, J. M. Gómez-Rodríguez, I. Brihuega, and F. Ynduráin, "Hydrogen physisorption channel on graphene: a highway for atomic h diffusion," 2D Materials **6**, 021004 (2019).

[51] A. Paris, N. Verbitskiy, A. Nefedov, Y. Wang, A. Fedorov, D. Haberer, M. Oehzelt, L. Petaccia, D. Usachov, D. Vyalikh, H. Sachdev, C. Wöll, M. Knupfer, B. Büchner, L. Calliari, L. Yashina, S. Irle, and A. Grüneis, "Kinetic isotope effect in the hydrogenation and deuteration of graphene," Adv. Funct. Mater. **23**, 1628–1635 (2013).

[52] M. M. S. Abdelnabi, E. Blundo, M. G. Betti, G. Cavoto, E. Placidi, A. Polimeni, A. Ruocco, K. Hu, Y. Ito, and C. Mariani, "Towards free-standing graphane: atomic hydrogen and deuterium bonding to nano-porous graphene," Nanotechnology **32**, 035707 (2021).

[53] R. Balog, B. Jørgensen, J. Wells, E. Lægsgaard, P. Hofmann, F. Besenbacher, and L. Hornekær, "Atomic hydrogen adsorbate structures on graphene," J. Am. Chem. Soc. **131**, 8744–8745 (2009).

[54] J. D. Thrower, B. Jørgensen, E. E. Friis, S. Baouche, V. Mennella, A. C. Luntz, M. Andersen, B. Hammer, and L. Hornekær, "Experimental evidence for the formation of highly super-hydrogenated polycyclic aromatic hydrocarbons through h atom addition and their catalytic role in h_2 formation," Astrophys. J. **752**, 3 (2012).

[55] L. Hornekær, Ž Šljivančanin, W. Xu, R. Otero, E. Rauls, I. Stensgaard, E. Lægsgaard, B. Hammer, and F. Besenbacher, "Metastable structures and recombination pathways for atomic hydrogen on the graphite (0001) surface," Phys. Rev. Lett. **96**, 156104 (2006).

[56] L. F. Huang, M. Y. Ni, G. R. Zhang, W. H. Zhou, Y. G. Li, X. H. Zheng, and Z. Zeng, "Modulation of the thermodynamic, kinetic, and magnetic properties of the hydrogen monomer on graphene by charge doping," J. Chem. Phys. **135**, 064705 (2011).

[57] M.-T. Nguyen and P. N. Phong, "Atomic transport at charged graphene: Why hydrogen and oxygen are so different," Chemistry Select **2**, 2797–2802 (2017).

[58] L. F. Huang, T. F. Cao, P. L. Gong, Z. Zeng, and C. Zhang, "Tuning the adatom-surface and interadatom interactions in hydrogenated graphene by charge doping," Phys. Rev. B **86**, 124533 (2012).

[59] Aleksandr V Marenich, Steven V Jerome, Christopher J Cramer, and Donald G Truhlar, "Charge model 5: An extension of hirshfeld population analysis for the accurate description of molecular interactions in gaseous and condensed phases," Journal of Chemical Theory and Computation **8**, 527–541 (2012).

[60] Y. Murata, A. Calzolari, and S. Heun, "Tuning hydrogen adsorption on graphene by gate voltage," J. Phys. Chem. C **122**, 11591–11597 (2018).